Istaroxime metabolite PST3093 selectively stimulates SERCA2a and reverses disease-induced changes in cardiac function

Martina Arici[a#], Mara Ferrandi[b#], Shih-Che Hsu[c], Eleonora Torre[a], Paolo Barassi[b], Andrea Luraghi[a], Carlotta Ronchi[a], Gwo-Jyh Chang[d], Francesco Peri[a], Patrizia Ferrari[b], Giuseppe Bianchi[b], Marcella Rocchetti[a*] and Antonio Zaza[a*]

[a]Department of Biotechnology and Biosciences, Università degli Studi di Milano-Bicocca, Milan, Italy.
[b]Windtree Therapeutics Inc., Warrington, Pennsylvania, USA.
[c]CVie Therapeutics Limited, Taipei, Taiwan.
[d]Chang Gung University, Tao-Yuan, Taiwan.

[#] MA and MF contributed equally as first authors to the article
*MR and AZ contributed equally as senior authors to the article

Corresponding authors:

Antonio Zaza, MD, FESC.
Dipartimento di Biotecnologie e Bioscienze
Università degli Studi di Milano-Bicocca
P.za della Scienza 2, 2016 Milano (IT)
antonio.zaza@unimib.it

Marcella Rocchetti, PhD.
Dipartimento di Biotecnologie e Bioscienze
Università degli Studi di Milano-Bicocca
P.za della Scienza 2, 2016 Milano (IT)
marcella.rocchetti@unimib.it

Abstract

Background. Heart failure (HF) therapeutic toolkit would strongly benefit from the availability of ino-lusitropic agents with a favorable pharmacodynamics and safety profile. PST3093 is the main metabolite of istaroxime, an agent combining Na^+/K^+ pump inhibition and SERCA2a stimulation, shown by phase 2 trials to be promising in the acute setting. PST3093 half-life is substantially longer than that of istaroxime; therefore, if it retained the effects of the parent compound, it would allow to exploit istaroxime pharmacodynamics in chronic treatment. **Methods and Results.** We studied PST3093 for its effects on SERCA2a and Na^+/K^+ ATPase activities, Ca^{2+} dynamics in isolated myocytes and hemodynamic effects in an *in-vivo* rat model of diabetic (streptozotocin (STZ)-induced) cardiomyopathy. At variance with its parent compound, PST3093 is a "selective" (i.e. devoid of Na^+/K^+ pump inhibition) SERCA2a activator. In *in-vivo* echocardiographic assessment, PST3093 improved overall cardiac performance (e.g. stroke volume) without decreasing heart rate, and reversed most STZ-induced abnormalities. Modulation of both systolic and diastolic indexes contributed to the improvement. For i.v. administration, PST3093 toxicity was considerably lower than that of istaroxime and its evaluation against 50 targets commonly involved in cardiac and extracardiac side-effects, failed to reveal significant interactions. **Conclusions.** PST3093 is a "selective" SERCA2a activator, the prototype of a novel pharmacodynamic category with a potential in the ino-lusitropic approach to HF, particularly with prevailing diastolic dysfunction. While PST3093 may actually contribute to the proven clinical efficacy of istaroxime, its pharmacodynamics are peculiar and its pharmacokinetics are suitable for chronic administration.

Keywords

istaroxime; metabolite; PST3093; heart failure; SERCA; inotropy-lusitropy.

Chemical compounds studied in this article: istaroxime (PubChem CID: 9841834); digoxin (PubChem CID: 2724385).

Abbreviations

AHF, acute heart failure; AP, action potential; APD, action potential duration; Ca_{rest}, resting Ca^{2+}; Ca_{SR}, sarcoplasmic reticulum Ca^{2+} content; CaT, Ca^{2+} transient; CO, cardiac output; CPA, cyclopiazonic acid; DT, deceleration time; E_{diast}, diastolic potential; EF, ejection fraction; ER, excitation-release; F_0, reference fluorescence; FS, fractional shortening; HF, heart failure; HR, heart rate; $I_{CaL,}$ L type Ca^{2+} current; I_{NaK}, Na^+/K^+ ATPase current; i.p., intraperitoneal administration; i.v., intravenous administration; IVSTd or IVSTs, interventricular septum thickness in diastole or systole; K_dCa,, Ca^{2+} dissociation constant , LD_{50}, *in vivo* dose causing 50% mortality; LV, left ventricle; LVEDD or LVESD, LV end-diastolic or systolic diameter; NCX, Na^+-Ca^{2+} exchanger; os, oral administration; PLN, phospholamban; PWTd or PWTs, posterior wall thickness in diastole or systole; SERCA, sarcoplasmic reticulum Ca^{2+} ATPase; SR, sarcoplasmic reticulum; STV, short term variability; STZ, streptozotocin; SV, stroke volume; SW, septal diastolic wall thickness; τ_{decay}, time-constant of Ca^{2+} decay; TDI, Tissue Doppler Imaging; V_{max}, maximal hydrolytic velocity

1. Introduction

Heart failure (HF) is characterized by abnormal Ca^{2+} distribution among subcellular compartments, which contributes to impaired contractility and relaxation[1], facilitates arrhythmias[2] and, in the long run, contributes to myocardial remodeling[3]. Deficient SERCA2a activity[4], often resulting from over inhibition by phospholamban (PLN)[5], mainly accounts for abnormal distribution of intracellular Ca^{2+}. Interventions currently available to modulate myocyte Ca^{2+} handling (e.g. amines, PDE inhibitors etc.) stimulate SERCA2a, but they do so in the context of a multi-target action, thus resulting in untoward effects. Selective SERCA2a enhancement would afford inotropic and lusitropic effects without the drawbacks of the multi-target action[2]. Accordingly, the use of SERCA2a stimulation in HF therapy is receiving considerable attention; nonetheless, for reasons other than refutation of the principle, none of these attempts has been successfully translated into the clinic. The only exception is istaroxime, a small-molecule drug, identified as SERCA2a enhancer by our group[6] and currently under clinical development for the treatment of acute HF[7,8]. Istaroxime has a double mechanism of action: it inhibits the Na^+/K^+ pump[9] and activates SERCA2a[6]. Thus, istaroxime increases overall cell Ca^{2+} content while promoting rapid Ca^{2+} sequestration into the sarcoplasmic reticulum (SR). Notably, at variance with Na^+/K^+ pump blockade alone, this neither facilitates spontaneous Ca^{2+} release from the SR[10], nor increases myocardial oxygen demand[11]. Thus, istaroxime may improve systolic and diastolic performance[7] without promoting arrhythmia or ischemia[8,12]. However, istaroxime has a very short half-life (t½ < 2,5 h after 24-hour infusion), resulting from both a very high hepatic clearance and extensive metabolism to a molecule, named PST3093, which has a much longer half-life (t½ 16h after 24-hour infusion) (Carubelli, unpublished results).

The present work aims to investigate whether PST3093 on its own may be endowed with pharmacological activity. To this end, PST3093 has been synthesized and studied in experimental set-ups at different levels of biological organization and in the context of disease-

induced dysfunction. PST3093 has been compared with istaroxime and digoxin as reference compounds.

2. Methods

Further detail on methods is given in the online supplement.

2.1. Animal model

All experiments involving animals confirmed to the guidelines for Animal Care endorsed by the Milano-Bicocca and Chang Gung Universities and to the Directive 2010/63/EU of the European Parliament on the protection of animals used for scientific purposes.

Streptozotocin (STZ)-induced diabetes was selected as a pathological model because of its association with reduced SERCA2a function[13] and relevance to diastolic dysfunction[14], for which a lusitropic action may be more relevant. Diabetes was induced in Sprague Dawley male rats (150-175 g) by a single i.v. streptozotocin (STZ group, 50 $mg \cdot kg^{-1}$) injection. Control (healthy group) rats received STZ vehicle (citrate buffer). Fasting glycaemia was measured after 1 week and rats with values >290 $mg \cdot dL^{-1}$ were considered diabetic [13]. Rats were euthanized by cervical dislocation under anesthesia with ketamine-xylazine (130-7.5 mg/kg i.p) 9 weeks after STZ injection.

2.2. Biochemical measurements

Total ATPase activity was assessed by measuring the rate of ^{32}P-ATP release ($\mu mol \cdot min^{-1}$) at 37°C.

2.2.1. Na^+/K^+ ATPase activity assay

The inhibitory effect of compounds was tested, at multiple concentrations, on suspensions of the enzyme α1 isoform from dog kidney. Na^+/K^+ ATPase activity was identified as the ouabain (1 mM)-sensitive component of total one; compound efficacy was expressed as the concentration exerting 50% inhibition (IC_{50}).

2.2.2. SERCA ATPase activity assay

Measurements were performed in whole tissue homogenates (rat) or in purified SR microsomes (guinea-pig). Cardiac preparations included SERCA2a and PLN. To test for PLN involvement in the effect of compounds, SERCA1 activity was measured in PLN-free microsomes (from guinea-pig skeletal muscle) before and after reconstitution with the PLN_{1-32} inhibitory fragment at a ratio of 300:1 for PLN:SERCA. The SERCA component, identified as the cyclopiazonic acid (CPA, 10 µM)-sensitive one, was measured at multiple Ca^{2+} concentrations (100-2000 nM)[15] and Ca^{2+} dose-response curves were fitted to estimate SERCA maximal hydrolytic velocity (V_{max}, $\mu mol \cdot min^{-1} \cdot mg^{-1}$ protein) and Ca^{2+} dissociation constant (K_dCa, nM). Either an increase of V_{max}, or a decrease of K_dCa (increased Ca^{2+} affinity) stand for enhancement of SERCA function.

2.2.3. PST3093 interaction with targets other than SERCA

To predict potential off-target actions of PST3093, its interaction with a panel of 50 ligands, potentially relevant to off-target effects, was carried out by Eurofins (Taiwan) on crude membrane preparations according to Eurofins described procedures. PST3093 was tested at the concentration of 10 µM.

2.3. Functional measurements in isolated myocytes

To ensure stabilization of drug effect, effects on functional parameters were analyzed after incubating cells with PST3093 or vehicle (control) for at least 30 min. Difference between means was thus tested by group comparison. All experiments were performed at 36.5 °C.

2.3.1. Na^+/K^+ ATPase current (I_{NaK})

I_{NaK} was recorded in isolated rat left ventricular (LV) myocytes as the holding current at -40 mV under conditions enhancing I_{NaK} and minimizing contamination by other conductances[13,16]. I_{NaK} inhibition by the compounds was expressed as percent reduction of ouabain (1 mM)-sensitive current; efficacy was expressed as the compound concentration exerting 50% inhibition (IC_{50}) effect.

2.3.2. Intracellular Ca^{2+} dynamics

Ca^{2+}-dependent fluorescence (Fluo 4-AM) was recorded in field stimulated (2 Hz) or patch-clamped rat LV myocytes and quantified by normalized units (F/F_0). Ca^{2+} dynamics was characterized through the properties of voltage-induced Ca^{2+} transients (CaT, amplitude and decay kinetics) and caffeine-induced ones, the latter estimating total SR Ca^{2+} content (Ca_{SR}). In patch-clamped myocytes, SR Ca^{2+} uptake rate was evaluated through a "SR loading" voltage protocol, specifically devised to examine the system at multiple levels of SR Ca^{2+} loading and to rule out Na^+/Ca^{2+} exchanger (NCX) contribution. Current through L-type Ca^{2+} channel (I_{CaL}) was simultaneously recorded and the excitation –release (ER) "gain" was calculated as the ratio between CaT amplitude and Ca^{2+} influx through I_{CaL} up to CaT peak[6] (protocol in Figure S1).

2.3.3. Electrical activity

Action potentials (APs) were recorded (I-clamp) from isolated guinea-pig LV myocytes, selected because of the AP similarity to the human one, under Tyrode superfusion. AP duration at 50% and 90% repolarization (APD_{50} and APD_{90}) and diastolic potential (E_{diast}) were measured 1) during steady state pacing at several rates; 2) dynamically upon stepping between two rates (APD adaptation). During steady pacing, short-term APD_{90} variability (STV) was calculated from 20-30 subsequent APD_{90} values according to Eq. 1[17]:

$$STV = \sum(|APD(n+1) - APDn|)/[nbeats * \sqrt{2}] \qquad \text{(Eq. 1)}$$

The kinetics of APD_{90} adaptation was quantified by the time constant (τ) of exponential data fitting.

***2.4. In-vivo* studies**

2.4.1. Acute drug toxicity in mice

Acute toxicity was evaluated by identifying the dose causing 50% mortality (LD_{50}, $mg \cdot kg^{-1}$ body weight) in male Albino Swiss CD-1 mice at 30 min after administration. LD_{50} was

compared between intravenous (i.v.) and oral (os) administration up to 250 $mg \cdot kg^{-1}$ iv and 200 $mg \cdot kg^{-1}$ respectively. Survival was also assessed at 24h.

2.4.2. Hemodynamic studies in rats with diabetic cardiomyopathy

Healthy and STZ rats were studied by transthoracic echocardiographic under urethane anesthesia (1.25 $g \cdot kg^{-1}$ i.p.). Left-ventricular end-diastolic (LVEDD) and end-systolic (LVESD) diameter, posterior wall (PWT) and interventricular septal (IVST) thickness were measured according to the American Society of Echocardiography guidelines[18]. Fractional shortening was calculated as FS = (LVEDD-LVESD)*$LVEDD^{-1}$. Trans-mitral flow velocity was measured (pulsed Doppler) to obtain early and late filling velocities (E, A waves) and E wave deceleration time (DT). DT was also normalized to E wave amplitude (DT/E ratio). Peak myocardial systolic (s') and diastolic velocities (e' and a'), were measured at the mitral annulus by Tissue Doppler Imaging (TDI).

Accordingly to our previous study[13], PST3093 was intravenously infused at 0.22 $mg \cdot kg^{-1}$ (0.16 ml/min); echocardiographic parameters were measured before and at 15 and 30 min during the infusion. Istaroxime (0.22 $mg \cdot kg^{-1}$) and digoxin (0.11 $mg \cdot kg^{-1}$), both infused for 15 min, were used as comparators.

2.5. Statistical analysis

Individual means were compared by unpaired *t*-test; multiple means were compared by one or two-way ANOVA for repeated measurements (RM); drug-induced changes in overall curve steepness were defined according to significance of the "factor X group" interaction. Data are reported as mean ± SEM; $p<0.05$ defined statistical significance of differences in all comparisons. Number of animals (N) and/or cells (n) are shown in each figure legend.

2.6. Chemicals

Istaroxime {PST2744: [E,Z]-3-[(2-aminoethoxy)imino]-androstane-6,17-dione hydrochloride} and its metabolite PST3093 {(E,Z)-[(6-beta-hydroxy-17-oxoandrostan-3-ylidene)amino]oxyacetic acid} were synthesized and produced at Prassis Research Institute

and Sigma-Tau Pharmaceutical Company and then by CVie Therapeutics Limited and WindTree Therapeutics. The batch of PST3093 utilized for *in-vitro* and *in-vivo* studies contained a 1:1 ratio of oxime E:Z isomers. Digoxin was purchased from Sigma-Aldrich.

3. Results

3.1. Chemical structure of PST3093

PST3093 is the final, long-lasting metabolite of istaroxime; its chemical structure is shown in Figure 1A. Compared to istaroxime, PST3093 retains the oxime moiety at position 3 with the amino-chain oxidized into a carboxylic chain, while the 6-keto group of istaroxime is stereo selectively reduced to a 6β-hydroxyl group.

3.2. Effect of PST3093 vs istaroxime on the Na^+/K^+ ATPase

3.2.1. Effect on Na^+/K^+ ATPase activity

Compounds were tested in a range of concentrations from 10^{-9} to 10^{-4} M (Figure 1B). Na^+/K^+ ATPase had a specific baseline activity of 14 $\mu mol \cdot min^{-1} \cdot mg^{-1}$ protein. The reference compound istaroxime inhibited Na^+/K^+ ATPase activity with IC_{50} values of $1.44 \pm 0.2*10^{-7}$ M; PST3093 did not inhibit the Na^+/K^+ ATPase activity up to 10^{-4} M, the maximal tested concentration.

3.2.2. Effect on Na^+/K^+ ATPase current (I_{NaK}) in cardiac myocytes

A sample I_{NaK} recording is shown in Figure 1C; I_{NaK} inhibition curves for PST3093 and istaroxime are shown in Figure 1D. The estimated IC_{50} for I_{NaK} inhibition by istaroxime was 32 ± 4 µM (modified from[13]); for PST3093 a 9.2 ± 1.1% reduction was observed at the limit concentration for solubility (100 µM), an effect that can be considered insignificant.

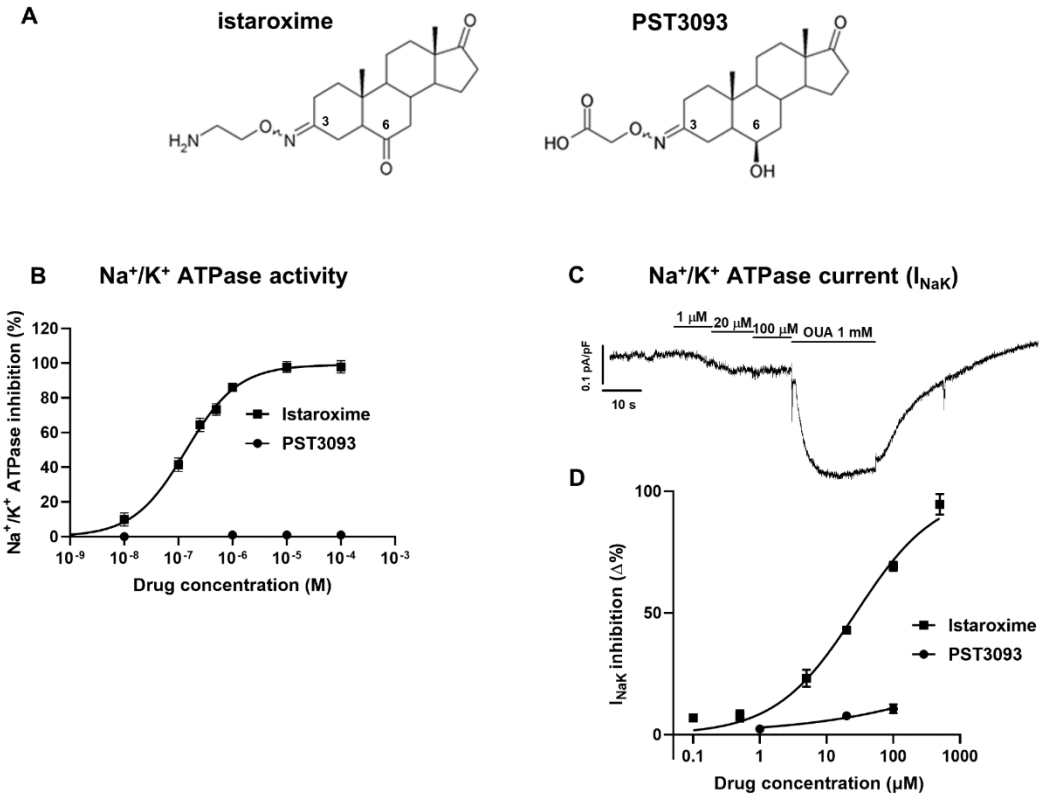

Figure 1. Modulation of Na^+/K^+ ATPase activity. A) Chemical structure of istaroxime and its metabolite PST3093. The main metabolic pathways of istaroxime are reduction of the carbonyl in position 6 catalyzed by carbonyl reductases and oxidative deamination of the primary amino group catalyzed by MAOs or tissue-bound semicarbazide-sensitive amine oxidase; **B)** inhibition of Na^+/K^+ ATPase activity by the two compounds in cardiac preparations (N=3); **C)** example of I_{NaK} measurement and its inhibition by PST3093 and ouabain (OUA as reference) in rat LV myocytes; **D**) concentration-response curves for I_{NaK} inhibtion by PST3093 (n=15) and istaroxime (modified from[13]).

3.3. Effect of PST3093 on SERCA ATPase activity

3.3.1. Effects on SERCA2a activity in normal and diseased myocardial preparations

In STZ rat preparations, baseline SERCA2a V_{max} was lower (by -27%) than in healthy ones, with no difference in K_dCa (Table S1), accordingly to our recent paper[13]. As also reported

previously[19], the analysis of compounds effects suggests a species-specific response of enzyme kinetics to modulation: whereas in rat preparations both PST3093 (Figure 2, Table S2) and istaroxime (Figure S2, Table S3) increased V_{max}, in guinea-pig ones the compounds decreased K_dCa instead (Table S3).

Over the whole range of concentration tested (0.1 - 1µM), PST3093 and istaroxime failed to affect ATPase Ca^{2+}-dependency in healthy rat preparations, but similarly increased V_{max} in STZ ones (e.g. +22% and +20%, respectively at 300 nM) with threshold at 100 nM and 300 nM for PST3093 and istaroxime, respectively. Thus, PST3093 and istaroxime displayed similar potency in ameliorating disease-induced depression of SERCA2a ATPase activity.

PST3093 and istaroxime effect was also detected in preparations from normal guinea-pig hearts, where they both reduced the K_dCa value by about 20% at 100 nM (Table S3).

To summarize, PST3093 and istaroxime equally stimulated SERCA2a ATPase activity in preparations including PLN**.** The effect was present in healthy guinea-pig preparations, but visible in rat ones only in the diseased state.

3.3.2. Dependency of SERCA stimulation by PST3093 on PLN

In a range of concentrations from 30 to 1000 nM, PST3093 (Figure 2E, Table S4) and istaroxime (Table S5) failed to affect SERCA1 activity in the absence of PLN. Reconstitution with the PLN_{1-32} fragment markedly reduced SERCA1 affinity for Ca^{2+} (K_dCa increased by 23-26%) (Figure 2F, Table S5). Under this condition, PST3093 dose-dependently reversed PLN-induced shift in K_dCa with an EC_{50} of 39 nM (Figure 2F). Istaroxime had a comparable effect, with an EC_{50} of 40 nM (Table S5).

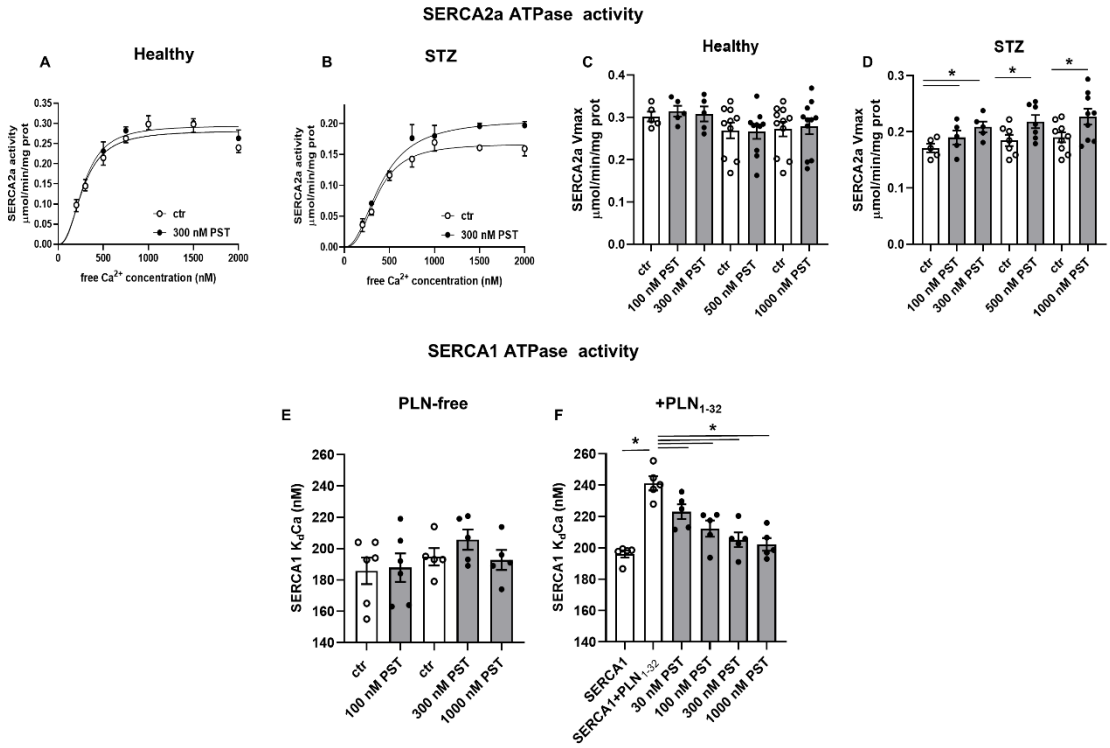

Figure 2. Modulation of SERCA ATPase activity in normal and diseased (STZ) preparations and its PLN-dependency. PST3093 effects were evaluated as modulation of the parameters (K_dCa and V_{max}) describing Ca^{2+} dependency of SERCA activity in myocardial homogenates or microsome preparations. **A)-B)** effect of PST3093 (300 nM) in cardiac homogenates from healthy and diabetic (STZ) rats; the parameter affected in this preparation was V_{max} (N=5, see Table S2 for K_dCa results). **C-D)** Concentration-dependency of V_{max} modulation by PST3093 in healthy and STZ rat preparations. Because in each experiment only two PST3093 concentrations have been tested, separate controls (ctr) are provided for low and high ones. N=5-11, * $p<0.05$ vs ctr (RM one-way ANOVA with post-hoc Tukey's multiple comparisons test or paired *t*-test). **E-F)** Concentration-dependency of PST3093 modulation of K_dCa in guinea-pig skeletal muscle microsomes containing SERCA1 alone (E) and after reconstitution with the PLN_{1-32} fragment (N=5). Data are the mean ± SEM. *$p<0.05$ (one-way ANOVA plus post-hoc Tukey's multiple comparisons).

3.4. PST3093 interaction with targets other than SERCA

The targets panel (50 items) included membrane receptors, key enzymes, ion channels and transporters, relevant to potential off-target cardiac and extracardiac effects (list in Table S6); PST3093 was tested at the concentration of 10 μM. None among the 50 items met criteria for significance of interaction. Thus, at least for the ligands shown in Table S6, no off-target action of PST3093 is expected.

3.5. PST3093 effects on intracellular Ca^{2+} dynamics in cardiac myocytes

3.5.1. Effect on intracellular Ca^{2+} dynamics under field-stimulation

Ca^{2+} dynamics were analysed in field stimulated (2 Hz, Figure 3A-B) rat LV myocytes isolated from healthy or STZ rats.

STZ myocytes had a lower SR Ca^{2+} content (Ca_{SR}) and a slower CaT decay than healthy ones, both compatible with reduced SERCA2a function; nonetheless CaT amplitude was not significantly reduced.

In healthy myocytes, 1 μM PST3093 failed to affect any of the Ca^{2+} dynamics parameters; in STZ-myocytes, PST3093 reduced the quiescence Ca^{2+} (Ca_{rest}) prior to caffeine application (Figure 3A-B) and partially restored Ca_{SR} and CaT decay. Moreover, the analysis of individual data points of Ca_{SR} indicates that, in STZ-myocytes, PST3093 restored the distribution of Ca_{SR} values peculiar of healthy ones. Taken together, these observations suggest that PST3093 by stimulating SERCA2a improved Ca^{2+} sequestration into the SR during quiescence.

3.5.2. Effect on SR Ca^{2+}uptake function in V-clamped myocytes

The "SR loading" protocol (see methods) was used to assess SR Ca^{2+} uptake under conditions emphasizing SERCA2a role. In STZ myocytes, as compared to healthy ones, SR reloading was significantly depressed (both in terms of CaT amplitude and ER gain) and CaT decay was slower at all time-points during reloading (Figure 3C-D). These changes are compatible with depressed SERCA2a function[13]. PST3093 (1 μM) was tested in STZ myocytes (Figure 3D),

where it sharply accelerated CaT decay, to restore the profile observed in healthy myocytes. Albeit less evident, drug-induced changes in CaT and ER gain point in the same direction. Overall, PST3093 restored SR function in diseased myocytes, most likely through SERCA2a enhancement, within the context of an intact cellular environment.

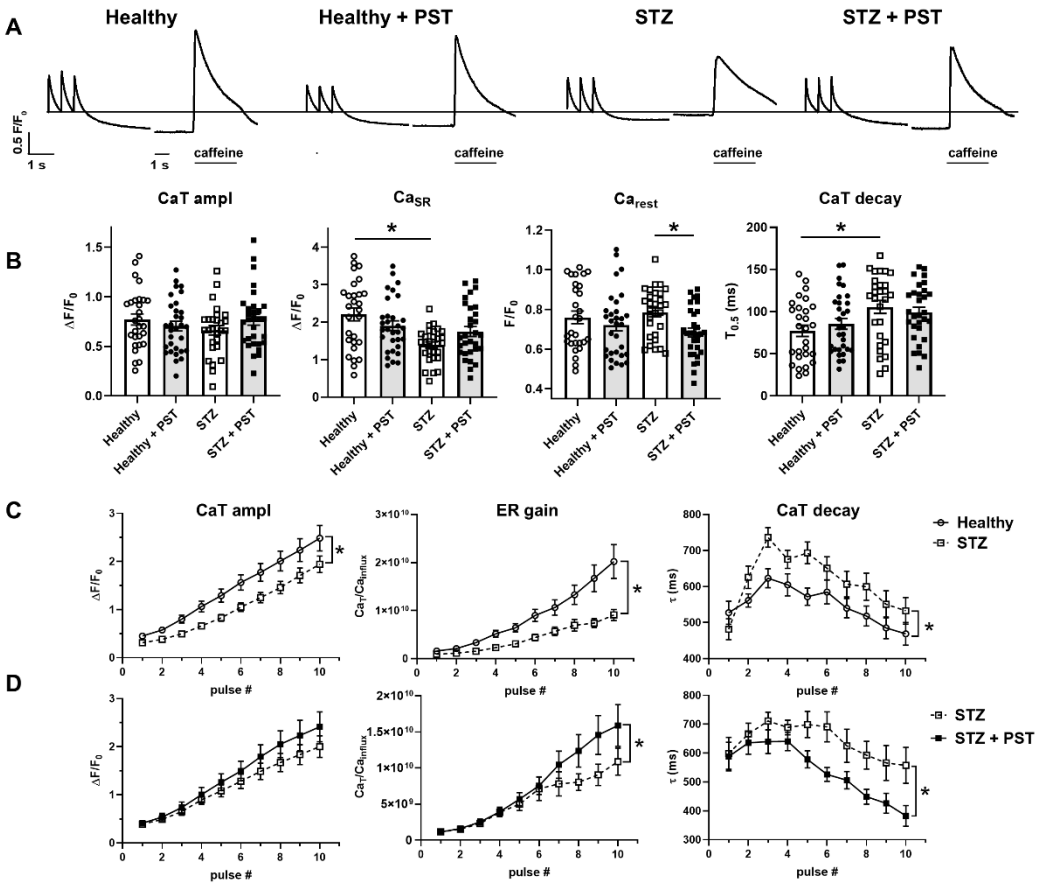

Figure 3. Modulation of intracellular Ca^{2+} handling in field stimulated (A-B) and patch-clamped (C-D) myocytes from healthy and diseased (STZ) hearts. A) Representative recordings of Ca^{2+} transients (CaT) triggered by steady-state electrical stimulation at 2Hz in intact cells, followed after 20 secs by caffeine-induced Ca^{2+} release measuring SR Ca^{2+} content (Ca_{SR}). PST3093 (1 µM) was tested in normal (healthy) and diseased (STZ) myocytes. **B)** Statistics for CaT amplitude, Ca_{SR}, time for 50% CaT decay ($T_{0.5}$), Ca^{2+} at pause end (Ca_{rest}). CTR N=3 (n=28 w/o PST3093, n=31 with PST3093), STZ N=4 (n=28 w/o PST3093, n=30 with PST3093). *$p<0.05$ (one-way ANOVA plus post-hoc Tukey's multiple comparisons). **C)**

Disease (STZ) effect on SR Ca^{2+} loading in patch-clamped myocytes. SR Ca^{2+} loading by a train of V- clamp pulses was initiated after caffeine-induced depletion; NCX was blocked by Na^{+} substitution to identify SERCA2a-specific effects (see Methods and Figure S1); myocytes from healthy (N=9, n=32) and diseased hearts (STZ, N=6, n=31) are compared. **D)** PST3093 effect in STZ myocytes (N=4, w/o PST3093 n=18, with PST3093, n=19). Panels from left to right: CaT amplitude, Excitation-Release (ER) gain (the ratio between CaT amplitude and Ca^{2+} influx through I_{CaL}), time constant (τ) of CaT decay. *p<0.05 for the "interaction factor" in two-way ANOVA for repeated measurements, indicating a different steepness of curves.

3.6. PST3093 effect on cellular electrical activity

PST3093 (100 nM) slightly reduced APD_{50} at all pacing rates, leaving the other AP parameters unchanged (Figure 4A-B). Notably, also steady-state APD rate-dependency and the kinetics of APD adaptation following a step change in rate, were unaffected by the agent (Figure 4C). STV of APD_{90}, a reporter of repolarization stability, was also unaffected by PST3093 (Figure 4D-E). Except for the absence of APD_{50} reduction, similar results were obtained with PST3093 at 1 μM (Figure S3).

The paucity of effects on the AP is consistent with the absence of hits in the analysis of PST3093 interaction (up to 10 μM) with molecular targets other than SERCA2a, among them ion channels and transporters (Table S6).

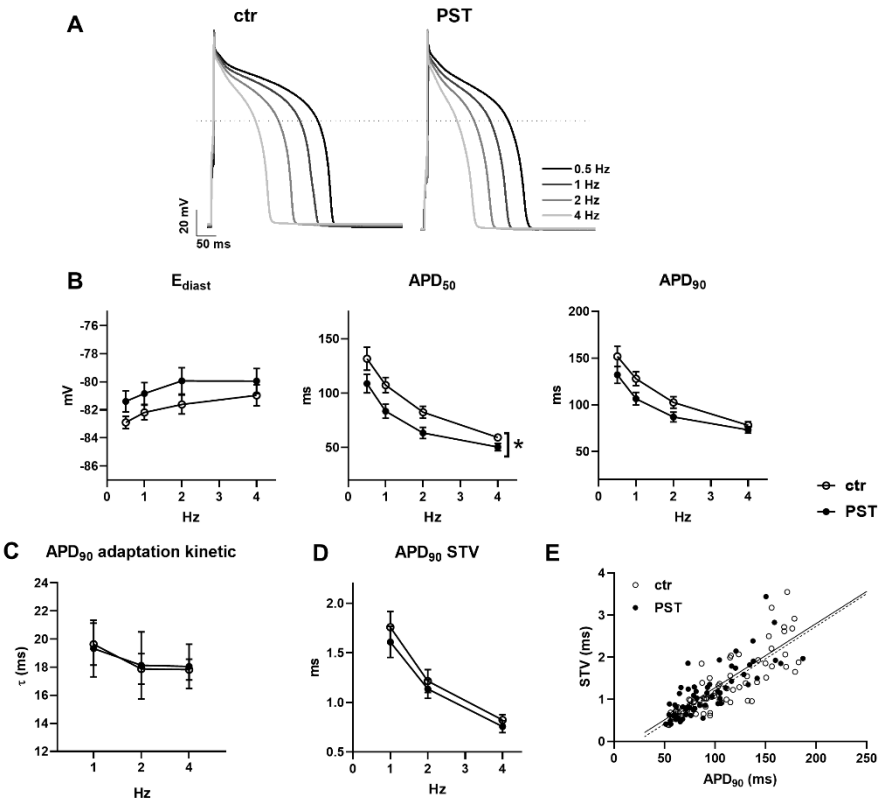

Figure 4. Modulation of electrical activity in guinea pig myocytes. The effect of PST3093 100 nM was tested on action potential (AP) parameters and their steady-state and dynamic rate-dependency in guinea pig myocytes (N=5). **A)** representative APs recorded at 0.5, 1, 2, 4 Hz in control (left) and with 100 nM PST3093 (right). **B)** Effect on the rate dependency of diastolic potential (E_{diast}) and AP duration (APD_{50}, APD_{90}) (n≥24 w/o PST3093, n≥22 with PST3093). **C)** Effect on the time constant (τ) of APD_{90} adaptation following a step change in rate (n≥22 w/o PST3093, n≥16 with PST3093). **D)** Effect on the rate-dependency of APD_{90} short term variability (STV) (n≥24 w/o PST3093, n≥20 with PST3093). **E)** Effect on the correlation between STV of APD_{90} and mean APD_{90}; data from 1, 2, 4 Hz were pooled. *$p<0.05$ for the "interaction factor" of two-way ANOVA for repeated measurements. The effect of PST3093 at a higher concentration (1 µM) is reported in Figure S3.

3.7. Acute toxicity in mice

The results are summarized in Table S7. For PST3093, LD_{50} values were >250 and >200 $mg \cdot kg^{-1}$ for i.v. and os administration, respectively. LD_{50} values for istaroxime were 30 $mg \cdot kg^{-1}$ for i.v. and 200 $mg \cdot kg^{-1}$ for os. Therefore, whereas PST3093 was 8-fold less toxic than istaroxime when administered i.v., oral toxicity was similar between the two compounds. For comparison with Na^+/K^+ ATPase blockade, digoxin LD_{50} values were also measured. Digoxin LD_{50} was 17 $mg \cdot kg^{-1}$ for i.v. administration, a value similar to that reported for oral one[20].

3.8. Modulation of cardiac function *in vivo* in rats with diabetic cardiomyopathy

Features of echo indexes of the STZ disease model are described first (Figure 5 Tables S9), followed by an account of drug effects in the same model (Figure 6, Table 1, Table S10).

3.8.1. Features of the disease model

Fasting hyperglycaemia, polydipsia, polyuria and polyphagia ensued 1 week after STZ injection; none of these symptoms was observed in healthy rats. Eight weeks after STZ, total BW was substantially lower in STZ rats; LV mass (by echo) was reduced in absolute value but, when normalized to BW, was not significantly different in STZ rats (Table S8).

Figure 5 and Table S9 compare echo indexes in healthy and STZ rats. Heart rate (HR) was lower in STZ rats (-20%; $p<0.05$) and stroke volume (SV) unchanged; nonetheless, differences in cardiac output (CO) between the two groups did not achieve significance. *Systolic indexes:* in STZ rats LV end-systolic diameter (LVESD) was larger and the ejection fraction (EF) reduced; fractional shortening (FS) and systolic tissue velocity (s') were depressed. *Diastolic indexes:* in STZ rats LV end-diastolic diameter (LVEDD) tended to be larger; peak E wave velocity (E) was slightly smaller and A wave velocity (A) was unchanged (E/A unchanged); E wave deceleration time (DT) was unchanged in absolute, but the DT/E ratio increased. Changes in early (e') and late (a') diastolic tissue velocities paralleled those in E and A waves; therefore, the e'/a' and E/e' ratios did not differ between STZ and healthy rats.

To summarize, in STZ rats echocardiographic abnormalities were rather subtle; nonetheless, 11 out of 21 indexes were significantly affected indicating derangements in both systolic and diastolic function.

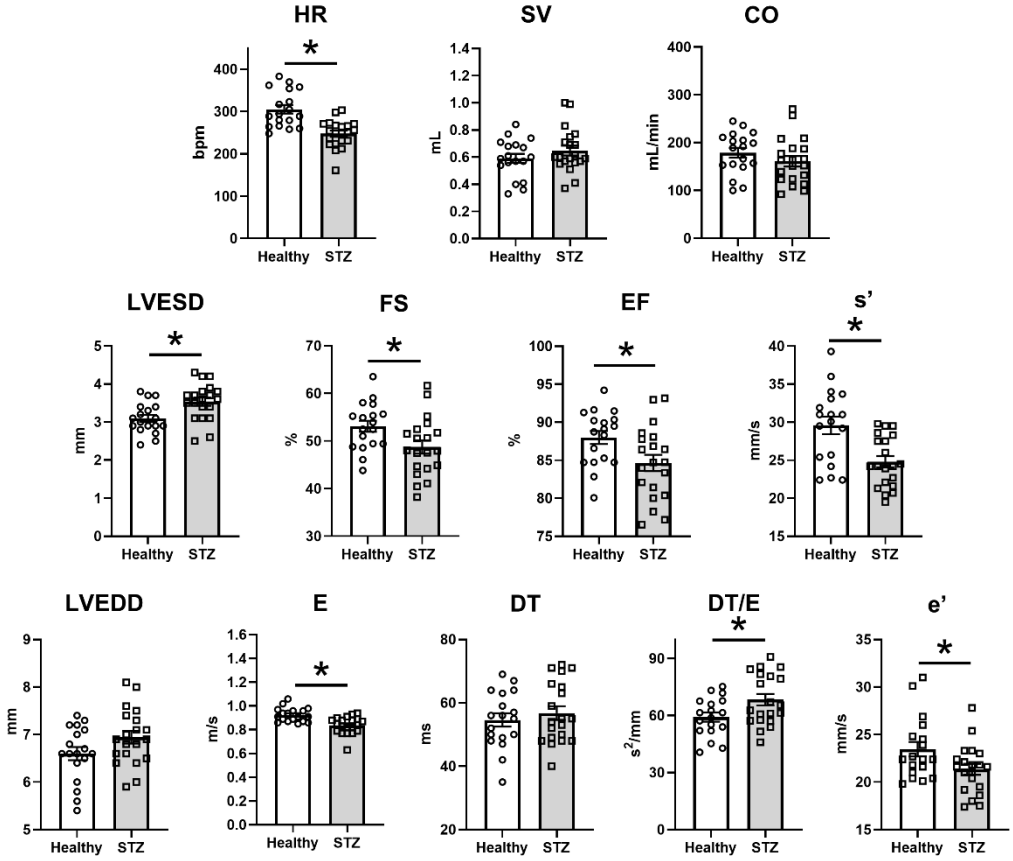

Figure 5. Disease (STZ) effect on *in-vivo* echocardiographic parameters. Echocardiographic parameters are compared between healthy rats (N=18) and 8 weeks after STZ treatment (N=20). Top row, global function parameters: HR: heart rate; SV: stroke volume; CO: cardiac output. Mid row, systolic function parameters: LVESD: left ventricular end-systolic diameter; FS: fractional shortening; EF: ejection fraction; s': peak systolic tissue velocity. Bottom row, diastolic function parameters: LVEDD: left ventricular end-diastolic diameter; E: E wave amplitude; DT: E wave deceleration time; DT/E: normalized DT; e': peak early diastolic tissue velocity. *p<0.05 (unpaired *t*-test).

3.8.2. Drug effects in the disease model

The effect of PST3093 (0.22 $mg \cdot kg^{-1} \cdot min^{-1}$) on echo indexes of STZ rats was investigated at 15 and 30 minutes of infusion (Figure 6 and Table S10). Data at 15 min were also obtained with istaroxime (0.22 $mg \cdot kg^{-1} \cdot min^{-1}$) and digoxin (0.11 $mg \cdot kg^{-1} \cdot min^{-1}$) (Table 1).

As shown in Figure S4 echo indexes values in the subset of STZ rats measured before PST3093 infusion were representative of the whole group used to define STZ effect. Overall, PST3093 increased SV volume and, albeit unchanged HR, it increased CO (Figure 6). *Systolic indexes*: PST3093 tended to decrease LVESD and increased FS, EF and s'. *Diastolic indexes*: PST3093 increased LVEDD, E, A and e' (E/A and E/e' unchanged, Table S10); DT and DT'/E were reduced. PST3093 effect was almost complete at 15 min of infusion, only minor increments were observed at 30 min (Figure 6). Collectively, PST3093 improved overall cardiac function, both systolic and diastolic, beyond simple recovery of STZ-induced derangements. As shown in Figure 6, PST3093 "reversed" STZ-induced changes in 7 out of 11 indexes; moreover, five additional indexes, unaffected by STZ, were changed by PST3093 in a direction compatible with positive inotropy/lusitropy (Table S10).

PST3093 effects were only partially shared by istaroxime (Table 1). Istaroxime failed to increase SV and systolic indexes (SV, FS, EF, s'); it increased CO but, at variance with PST3093, this was because HR increased. Similar to PST3093, istaroxime shortened DT, DT/E and increased e', a' and A; however, it did not change E, thus reducing E/e'.

Digoxin (Table 1), as expected from its inotropic effect, increased systolic indexes (FS, EF and s'); however, at variance with PST3093, it did not affect SV or CO. Notably, also digoxin improved diastolic function to some extent: E/A, DT and DT/E were reduced and e' was increased.

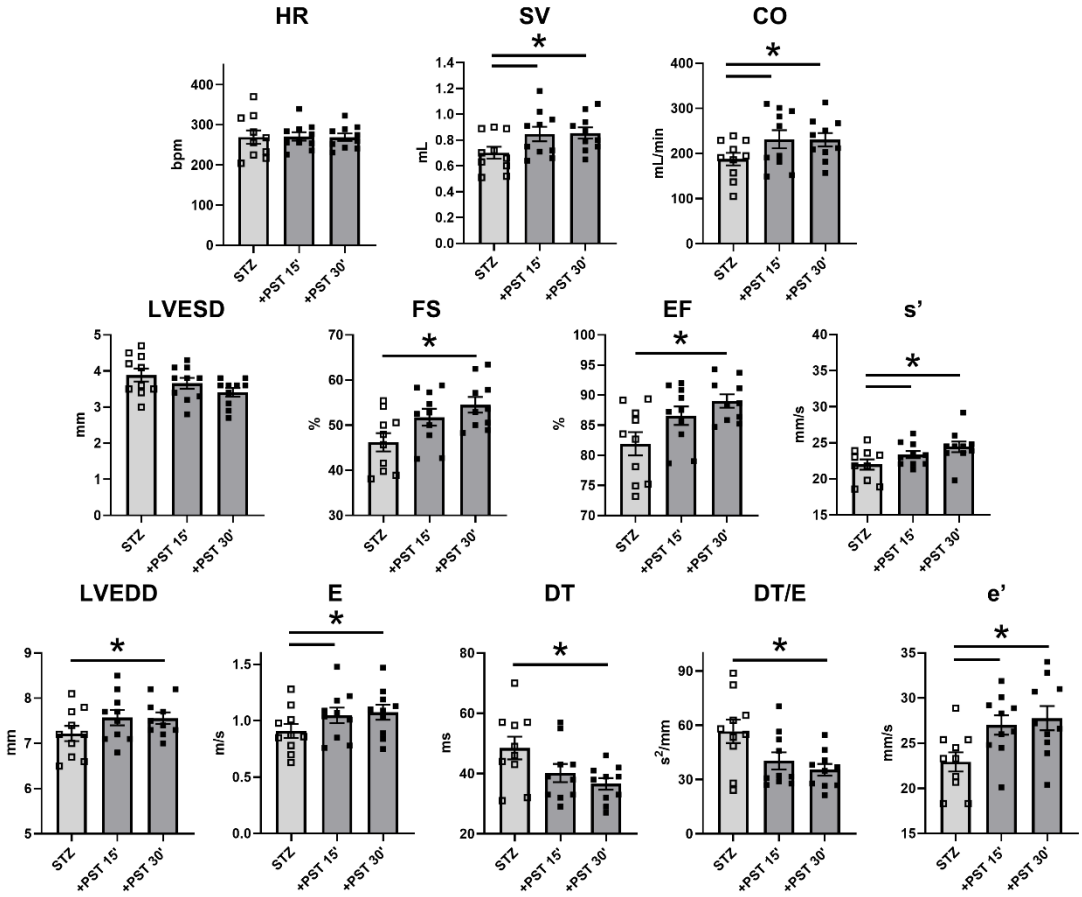

Figure 6. PST3093 effect on *in-vivo* echocardiographic parameters in diseased (STZ) rats. PST3093 was intravenously infused (0.22 $mg.kg^{-1}.min^{-1}$) in rats 8 weeks after STZ treatment. Echocardiographic parameters were measured before and at 15 and 30 min during drug infusion. Rows and symbols as in Figure 5; N=10 rats; *$p<0.05$. The effects of PST3093 on all echocardiographic parameters of STZ rats are reported in Table S10.

Table 1: Effects of istaroxime, PST3093 and digoxin on echo indexes of STZ rats at 15 minutes of infusion.

Echo parameters		Istaroxime 0,22 mg/kg/min		PST3093 0,22 mg/kg/min		Digoxin 0,11 mg/kg/min	
		before	after 15 min	before	after 15 min	before	after 15 min
Morphometric parameters	IVSTd (mm)	1,91±0,09	1,97±0,16	1,89±0,09	1,86±0,11	1,79±0,07	1,81±0,04
	PWTd (mm)	1,6±0,07	1,68±0,09	1,46±0,05	1,47±0,07	1,71±0,08	1,66±0,1
	LVEDD (mm)	7,25±0,15	7,1±0,2	7,22±0,17	7,57±0,17	6,76±0,15	6,67±0,15
	IVSTs (mm)	2,4±0,1	2,45±0,12	2,16±0,11	2,31±0,13	2,25±0,14	2,31±0,1
	PWTs (mm)	2,33±0,16	2,42±0,15	2,43±0,12	2,62±0,14	2,47±0,16	2,68±0,14
	LVESD (mm)	3,82±0,21	3,8±0,2	3,89±0,18	3,66±0,15	3,53±0,17	3,14±0,14 #
Systolic parameters	FS (%)	47,21±2,4	46,72±2,1	46,2±2,02	51,8±1,89 #	47,62±1,9	53,09±1,8 #
	s' (mm/s)	23,37±0,9	23,05±0,7	22,0±0,72	23,4±0,5 #	23,5±0,9	26±1,5 #
	EF (%)	83 ± 2	82 ± 62	82 ± 1,9	87 ± 1,5 #	84±1,5	88±1,3 #
Diastolic parameters	E (mm/s)	0,91±0,04	0,94±0,04	0,91±0,06	1,05±0,07 #	0,831±0,03	0,924±0,06
	A (mm/s)	0,66±0,04	0,78±0,05 #	0,79±0,08	0,87±0,07	0,59±0,05	0,79±0,05 #
	E/A	1,39±0,06	1,22±0,08	1,18±0,05	1,22±0,04	1,48±0,11	1,2±0,06 #
	DT (ms)	46,62±4,1	34,12±2,5 #	48,5±3,8	40,2±3,0	53,4±3,8	44,1±3,2 #
	DT/E	51,91±4,9	36,66±3,3 #	56,7±6,5	40,39±4,8 #	65,21±5,3	50,18±5,4 #
	E/DT	21,28±3,2	28,98±2,8 #	20,61±3,0	27,51±2,6 #	16,53±1,7	22,66±3,0
	e' (mm/s)	21,23±0,99	24,73±0,61 #	22,94±1,0	27,01±1,1 #	20,9±0,5	23,8±0,9 #
	a' (mm/s)	27,61±1,9	31,35±1,5 #	28,72±2,2	31,06±1,5	25,9±1,9	29,8±1,9
	e'/a'	0,78±0,04	0,79±0,03	0,83±0,06	0,88±0,04	0,85±0,06	0,82±0,04
	E/e'	43,6±2,6	38,29±1,6 #	39,5±1,7	38,61±1,5	39,64±0,9	38,95±2,3
Overall cardiac function	HR (bpm)	266,2±9,8	316,2±7,5 #	270±17	271±10	236±12	257±11
	SV (ml)	0,71±0,04	0,67±0,05	0,702±0,05	0,847±0,06 #	0,589±0,03	0,601±0,04
	CO (ml/min)	188,8±10,5	211,2±13,2 #	187,7±13,7	231,7±20,2 #	138,5±11,2	155,6±14,4
	N	8	8	10	10	10	10

4. Discussion

In the present study, we have investigated effects of PST3093, the long-lasting metabolite of istaroxime, at molecular, cellular and *in-vivo* levels. The interest in this molecule is motivated by 1) the possibility that it may actually contribute to (i.e. be endowed with) the unique mechanism of action and interesting therapeutic profile of istaroxime (inotropy and lusitropy at low proarrhythmic risk, confirmed in phase 2 clinical trials)[7,8,11,12] and 2) the possibility it would afford to test the clinical benefit associated specifically with the rescue of SERCA2a depression, which is widely recognized as the basis for many among HF abnormalities.

PST3093 effect has been tested in three experimental settings with incremental level of biological organization, including *in-vivo* measurements from diseased hearts. The consistency of effects across these three sets of experiments confers robustness to the findings.

The results of molecular studies indicate that PST3093 differs from istaroxime because it is devoid of any inhibitory activity on the Na^+/K^+ ATPase, while retaining SERCA2a stimulatory activity in diseased preparations. This identifies PST3093 as a "selective" SERCA2a activator. SERCA alone (SERCA1) was insensitive to PST3093, but sensitivity was restored by its reconstitution with the PLN soluble fragment. Thus, similar to istaroxime[19], PST3093 may act by weakening SERCA-PLN interaction. In rat preparations, PST3093 (and istaroxime) increased SERCA2a V_{max}. Albeit this apparently conflicts with the notion that interference with PLN should decrease the K_dCa instead[21], the same pattern coexisted with evidence, by several independent approaches, of istaroxime antagonism of SERCA2a-PLN interaction[19]. The reason for this apparent discrepancy is unclear; the observation that PST3093 effect on SR Ca^{2+} uptake was present in rat cardiac myocytes (i.e. at physiological Ca^{2+} concentrations) suggests that it may reside in specificities of the microsomal preparation.

Investigations in intact ventricular myocytes confirm a negligible effect of PST3093 on Na^+/K^+ pump function. Furthermore, PST3093 abolished STZ-induced intracellular Ca^{2+} abnormalities likely dependent on SERCA2a downregulation. While PST3093 clearly stimulated SR Ca^{2+}

uptake under V-clamp conditions (Figure 3C-D), it failed to clearly affect CaT decay kinetic and Ca_{SR} content in field-stimulated myocytes (Fig 3A-B). This apparent discrepancy may result from failure to control the AP profile during field-stimulation measurements as previously described[13]. Overall, results in isolated myocytes are consistent with SERCA2a activation and suggest that it may indeed occur at physiological Ca^{2+} concentrations.

The present *in-vivo* studies were conducted by echocardiography in a disease model characterized by impairment of SERCA2a function[13,22]. In this model, PST3093 infusion improved overall cardiac performance (SV and CO); both systolic and diastolic indexes were positively affected by the agent. Mechanistic interpretation of echocardiographic indexes is often ambiguous. For instance, both DT prolongation and shortening have been associated with deterioration of diastolic function[11,23]. These puzzling observations can be interpreted by considering the contribution to DT of opposing factors, each prevailing in a specific condition[24]. At any rate, whenever HF was associated with DT shortening, istaroxime (having PST3093 as a metabolite) prolonged it[7,11]. A further difficulty may arise from the expectation that ino-lusitropy may increase atrial contraction (A amplitude) and ventricular relaxation (E amplitude) at the same time, thus conceivably making their ratio (E/A) unable to detect drug effects on diastolic function. An approach to the interpretation of drug effects, independent of mechanistic models, is to check whether the drug counters disease-induced abnormalities. In the case of PST3093, this was true for the majority of indexes (7 out of 11), the most notable exception being a small further increase in LVEDD. While increments in LVEDD are usually associated with deterioration of systolic function, PST3093 tended to decrease LVESD instead. The LVEDD increment was indeed associated with increased SV, and EF to which it likely contributed.

With the exception of guinea-pig, PST3093 efficacy on SERCA2a function in the diseased condition consistently contrasted with the lack of effect in healthy preparations (Figures 2 and 3). This suggests that SERCA2a function, while not strictly limiting in health, may become so

whenever its "reserve" is diminished. This view may not clash with the clear-cut effect of PLN knock-out in healthy murine myocytes; indeed, SERCA2a modulation by PST3093 may be, albeit functionally significant, subtler than complete PLN ablation.

While failing to increase the amplitude of CaT, PST3093 improved echo indexes of systolic function. Mechanisms at two levels may account for this observation: at the intracellular level, increased compartmentation of Ca^{2+} within the SR may improve the energetic efficiency of Ca^{2+} cycling[25]; at the organ level, improved relaxation may increase preload, with its well-known impact on systolic force[26]. Indeed, normalization of diastolic function in HF patients with preserved ejection fraction, may restore cardiac output irrespective of changes in the latter[27]. On the other hand, digoxin, whose mechanism of action is purely inotropic, accelerated early relaxation (DT shortening and e' increase). This is consistent with systo-diastolic coupling, i.e. the contribution to early relaxation of elastic restitution (recoil) of systolic force[28].

Whereas istaroxime LD_{50} was lower following i.v. than oral administration in mice, PST3093 toxicity was roughly similar between the two routes and remarkably lower than that of i.v. istaroxime. This suggests that PST3093 does not share a component of istaroxime activity, with high impact on toxicity, which is eliminated by hepatic first-pass metabolism; based on the present results, we speculate that it may consist of Na^+/K^+ pump inhibition. Absence of interaction with 50 cardiac and non-cardiac targets commonly involved in drug toxicity provides at least a first level evidence of PST3093 suitability as a therapeutic agent.

4.1. Limitations

Whereas, in the *in-vivo* experiments PST3093 effects generally achieved a maximum at 30 min of infusion, istaroxime infusion period was limited to 15 min. Our previous study[13] indicates that a 15 min infusion is sufficient for modulation of diastolic parameters by istaroxime. This time-point was selected in the present study to minimize metabolism to PST3093, thus allowing it to differentiate istaroxime's own effect from that of its metabolite. Nonetheless, istaroxime

effects reported here might differ from the steady-state ones, described in previous studies[7,8,11], to which PST3093 (the metabolite) might actually contribute.

Translation of the present *in-vivo* results to human therapy has to consider differences between clinical HF and the STZ rat model, which has specific hemodynamic features[29]. However, consistency of the istaroxime effect reported here with that described in HF patients[8] supports this translation.

4.2. Therapeutic relevance and perspective

The results of this study identify PST3093 as a prototype "selective" (i.e. devoid of Na^+/K^+ pump inhibition) SERCA2a activator. This may entail significant differences from the already characterized pharmacodynamic profile of istaroxime.

In the case of istaroxime, lack of the proarrhythmic effect (expected from Na^+/K^+ ATPase inhibition[6]) is likely due to SERCA2a stimulation. Indeed, the latter may reduce the occurrence of "Ca^{2+} waves" and the resulting "triggered activity"[2,30,31]. It is logical to predict that a pure SERCA2a activator may exert substantial antiarrhythmic effects, at least under the common conditions characterized by SR instability (e.g. HF). On the other hand, Na^+/K^+ pump inhibition may contribute to inotropy; thus, at least theoretically, PST3093 is expected to increase systolic force less than istaroxime. The present results argue for a PST3093 effect on global cardiac function, including positive inotropy, which was partly unexpected. Nonetheless, as detailed in Limitations, comparison with istaroxime within the present setting may be confounding.

Beside affording inotropy and lusitropy, SERCA2a stimulation may improve intracellular Ca^{2+} compartmentalization, with potential long-term effects on energetic efficiency and biology of cardiac myocytes[2]. This may be highly relevant for PST3093, which has a half-life of 16 hours (Carubelli, unpublished), compatible with oral (chronic) administration. However, chronic usage of PST3093 can still be hindered by the persistence of the oxime moiety, which entails a potential genotoxic effect; efforts are ongoing to obtain oxime-free PST3093 derivatives retaining SERCA2a stimulatory action. On the other hand, considering the low incidence and

entity of side-effects after acute infusion of its parent compound, other types of toxicity preventing PST3093 therapeutic use are unlikely. This view is reinforced by the lack of effects on cellular electrophysiology and of off-target interactions.

4.3. Conclusions

HF treatment would strongly benefit from the availability of ino-lusitropic agents with a favorable profile. PST3093 is the main metabolite of istaroxime showing a longer half-life in human circulation compared to parent drug, activates SERCA2a, doesn't inhibit Na^+-K^+ ATPase and improves systolic and diastolic performance in a model of diabetic cardiomyopathy. Overall, PST3093 acting as "selective" SERCA2a activator can be considered the prototype of a novel pharmacodynamic category for the ino-lusitropic approach of HF.

Declaration of interest

MF and PB are Windtree employees, PF and GB are Windtree consultants, S-CH is an employee of CVie Therapeutics Limited. All the other Authors declare no conflict of interest.

Funding

This work was supported by CVie Therapeutics Limited (Taipei, Taiwan), WindTree Therapeutics (Warrington, USA) and University of Milano Bicocca.

Supplementary material

Supplementary data associated with this article are reported in the Online Supplement.

References

1. Bers DM, Despa S. Cardiac myocytes Ca2+ and Na+ regulation in normal and failing hearts. *J Pharmacol Sci* 2006;**100**:315–322.

2. Zaza A, Rocchetti M. Calcium Store Stability as an Antiarrhythmic Endpoint. *Curr Pharm Des* 2015;**21**:1053–1061.

3. Nakayama H, Chen X, Baines CP, Klevitsky R, Zhang X, Zhang H, Jaleel N, Chua BHL, Hewett TE, Robbins J, Houser SR, Molkentin JD. Ca2+- and mitochondrial-dependent cardiomyocyte necrosis as a primary mediator of heart failure. *J Clin Invest* 2007;**117**:2431–2444.

4. Minamisawa S, Hoshijima M, Chu G, Ward CA, Frank K, Gu Y, Martone ME, Wang Y, Ross J, Kranias EG, Giles WR, Chien KR. Chronic phospholamban-sarcoplasmic reticulum calcium atpase interaction is the critical calcium cycling defect in dilated cardiomyopathy. *Cell* 1999;**99**:313–322.

5. Kranias EG, Hajjar RJ. Modulation of cardiac contractility by the phopholamban/SERCA2a regulatome. *Circ Res* 2012;**110**:1646–1660.

6. Rocchetti M, Besana A, Mostacciuolo G, Micheletti R, Ferrari P, Sarkozi S, Szegedi C, Jona I, Zaza A. Modulation of sarcoplasmic reticulum function by Na+/K + pump inhibitors with different toxicity: Digoxin and PST2744 [(E,Z)-3-((2-aminoethoxy)imino)androstane-6,17-dione hydrochloride]. *J Pharmacol Exp Ther* 2005;**313**:207–215.

7. Shah SJ, Blair JEA, Filippatos GS, MacArie C, Ruzyllo W, Korewicki J, Bubenek-Turconi SI, Ceracchi M, Bianchetti M, Carminati P, Kremastinos D, Grzybowski J, Valentini G, Sabbah HN, Gheorghiade M. Effects of istaroxime on diastolic stiffness in acute heart failure syndromes: Results from the Hemodynamic, Echocardiographic, and Neurohormonal Effects of Istaroxime, a Novel Intravenous Inotropic and Lusitropic Agent: A Randomized Controlled Trial in P. *Am Heart J* 2009;**157**:1035–1041.

8. Carubelli V, Zhang Y, Metra M, Lombardi C, Felker GM, Filippatos G, O'Connor CM, Teerlink JR, Simmons P, Segal R, Malfatto G, Rovere MT La, Li D, Han X, Yuan Z,

Yao Y, Li B, Lau LF, Bianchi G, Zhang J. Treatment with 24 hour istaroxime infusion in patients hospitalised for acute heart failure: a randomised, placebo-controlled trial. *Eur J Heart Fail* 2020;**22**:1684–1693.

9. Micheletti R, Mattera GG, Rocchetti M, Schiavone A, Loi MF, Zaza A, Gagnol RJP, Munari S De, Melloni P, Carminati P, Bianchi G, Ferrari P. Pharmacological profile of the novel inotropic agent (E,Z)-3-((2-aminoethoxy)imino)androstane-6,17-dione hydrochloride (PST2744). *J Pharmacol Exp Ther* 2002;**303**:592–600.

10. Alemanni M, Rocchetti M, Re D, Zaza A. Role and mechanism of subcellular Ca2+ distribution in the action of two inotropic agents with different toxicity. *J Mol Cell Cardiol* 2011;**50**:910–918.

11. Sabbah HN, Imai M, Cowart D, Amato A, Carminati P, Gheorghiade M. Hemodynamic Properties of a New-Generation Positive Luso-Inotropic Agent for the Acute Treatment of Advanced Heart Failure. *Am J Cardiol* 2007;**99**:41A-46A.

12. Gheorghiade M, Blair JEA, Filippatos GS, Macarie C, Ruzyllo W, Korewicki J, Bubenek-Turconi SI, Ceracchi M, Bianchetti M, Carminati P, Kremastinos D, Valentini G, Sabbah HN. Hemodynamic, Echocardiographic, and Neurohormonal Effects of Istaroxime, a Novel Intravenous Inotropic and Lusitropic Agent. A Randomized Controlled Trial in Patients Hospitalized With Heart Failure. *J Am Coll Cardiol* 2008;**51**:2276–2285.

13. Torre E, Arici M, Lodrini AM, Ferrandi M, Barassi P, Hsu S-C, Chang G-J, Boz E, Sala E, Vagni S, Altomare C, Mostacciuolo G, Bussadori C, Ferrari P, Bianchi G, Rocchetti M. SERCA2a stimulation by istaroxime improves intracellular Ca2+ handling and diastolic dysfunction in a model of diabetic cardiomyopathy. *Cardiovasc Res* 2021; doi: 10.1093/cvr/cvab123.

14. Valero-Muñoz M, Backman W, Sam F. Murine Models of Heart Failure With Preserved

Ejection Fraction: A “Fishing Expedition”. *JACC Basic to Transl Sci* 2017;**2**:770–779.

15. Micheletti R, Palazzo F, Barassi P, Giacalone G, Ferrandi M, Schiavone A, Moro B, Parodi O, Ferrari P, Bianchi G. Istaroxime, a Stimulator of Sarcoplasmic Reticulum Calcium Adenosine Triphosphatase Isoform 2a Activity, as a Novel Therapeutic Approach to Heart Failure. *Am J Cardiol* 2007;**99**:24A-32A.

16. Rocchetti M, Besana A, Mostacciuolo G, Ferrari P, Micheletti R, Zaza A. Diverse toxicity associated with cardiac Na+/K+ pump inhibition: Evaluation of electrophysiological mechanisms. *J Pharmacol Exp Ther* 2003;**305**:765–771.

17. Altomare C, Bartolucci C, Sala L, Bernardi J, Mostacciuolo G, Rocchetti M, Severi S, Zaza A. IKr Impact on Repolarization and Its Variability Assessed by Dynamic Clamp. *Circ Arrhythmia Electrophysiol* 2015;**8**:1265–1275.

18. Lang RM, Bierig M, Devereux RB, Flachskampf FA, Foster E, Pellikka PA, Picard MH, Roman MJ, Seward J, Shanewise J, Solomon S, Spencer KT, St John Sutton M, Stewart W. American Society of Echocardiography’s Nomenclature and Standards Committee; Task Force on Chamber Quantification; American College of Cardiology Echocardiography Committee; American Heart Association; European Association of Echocardiography; European So. *Eur J Echocardiogr* 2006;**7**:79–108.

19. Ferrandi M, Barassi P, Tadini-Buoninsegni F, Bartolommei G, Molinari I, Tripodi MG, Reina C, Moncelli MR, Bianchi G, Ferrari P. Istaroxime stimulates SERCA2a and accelerates calcium cycling in heart failure by relieving phospholamban inhibition. *Br J Pharmacol* 2013;**169**:1849–1861.

20. Georges A, Page J, Duvernay G. Biological activity of formyl derivatives of digitalis glycosides. *Arch Int Pharmacodyn thérapie* 1965;**153**:436–449.

21. Brittsan AG, Ginsburg KS, Chu G, Yatani A, Wolska BM, Schmidt AG, Asahi M, MacLennan DH, Bers DM, Kranias EG. Chronic SR Ca2+-ATPase inhibition causes

adaptive changes in cellular Ca2+ transport. *Circ Res* 2003;**92**:769–776.

22. Choi KM, Zhong Y, Hoit BD, Grupp IL, Hahn H, Dilly KW, Guatimosim S, Jonathan Lederer W, Matlib MA. Defective intracellular Ca2+ signaling contributes to cardiomyopathy in type 1 diabetic rats. *Am J Physiol - Hear Circ Physiol* 2002;**283**:H1398–H1408.

23. Eren M, Gorgulu S, Uslu N, Celik S, Dagdeviren B, Tezel T. Relation between aortic stiffness and left ventricular diastolic function in patients with hypertension, diabetes, or both. *Heart* 2004;**90**:37–43.

24. Mossahebi S, Zhu S, Kovács SJ. Fractionating E-wave deceleration time into its stiffness and relaxation components distinguishes pseudonormal from normal filling. *Circ Cardiovasc Imaging* 2015;**8** doi: 10.1161/CIRCIMAGING.114.002177.

25. Shannon TR, Chu G, Kranias EG, Bers DM. Phospholamban Decreases the Energetic Efficiency of the Sarcoplasmic Reticulum Ca Pump. *J Biol Chem* 2001;**276**:7195–7201.

26. Shiels HA, White E. The Frank-Starling mechanism in vertebrate cardiac myocytes. *J Exp Biol* 2008;**211**:2005–2013.

27. Tobushi T, Nakano M, Hosokawa K, Koga H, Yamada A. Improved diastolic function is associated with higher cardiac output in patients with heart failure irrespective of left ventricular ejection fraction. *J Am Heart Assoc* 2017;**6**:doi: 10.1161/JAHA.116.003389.

28. Burns AT, Gerche A La, Prior DL, MacIsaac AI. Left Ventricular Untwisting Is an Important Determinant of Early Diastolic Function. *JACC Cardiovasc Imaging* 2009;**2**:709–716.

29. Mihm MJ, Seifert JL, Coyle CM, Bauer JA. Diabetes related cardiomyopathy time dependent echocardiographic evaluation in an experimental rat model. *Life Sci* 2001;**69**:527–542.

30. Bai Y, Jones PP, Guo J, Zhong X, Clark RB, Zhou Q, Wang R, Vallmitjana A, Benitez R, Hove-Madsen L, Semeniuk L, Guo A, Song LS, Duff HJ, Chen SRW. Phospholamban knockout breaks arrhythmogenic Ca2+ waves and suppresses catecholaminergic polymorphic ventricular tachycardia in mice. *Circ Res* 2013;**113**:517–526.

31. Fernandez-Tenorio M, Niggli E. Stabilization of Ca2+ signaling in cardiac muscle by stimulation of SERCA. *J Mol Cell Cardiol* 2018;**119**:87–95.